SNLS-03D3bb – a super-Chandrasekhar mass Type Ia supernova

D. Andrew Howell[1], Mark Sullivan[1], Peter E. Nugent[2], Richard S. Ellis[3], Alexander J. Conley[1], Damien Le Borgne[4], Raymond G. Carlberg[1], Julien Guy[5], David Balam[6], Stephane Basa[7], Dominique Fouchez[8], Isobel M. Hook[9], Eric Y. Hsiao[6], James D. Neill[6], Reynald Pain[5], Kathryn M. Perrett[1], Christopher J. Pritchet[6]

[1]*Department of Astronomy and Astrophysics, University of Toronto, 60 St. George Street, Toronto, ON M5S 3H8, Canada*

[2]*Lawrence Berkeley National Laboratory, Mail Stop 50-232, 1 Cyclotron Road, Berkeley CA 94720 USA*

[3]*California Institute of Technology, E. California Blvd., Pasadena, CA 91125, USA*

[4]*DAPNIA/Service d'Astrophysique, CEA/Saclay, 91191 Gif-sur-Yvette Cedex, France*

[5]*LPNHE, CNRS-IN2P3 and University of Paris VI & VII, 75005 Paris, France*

[6]*Department of Physics and Astronomy, University of Victoria, PO Box 3055, Victoria, BC V8W 3P6, Canada*

[7]*LAM CNRS, BP8, Traverse du Siphon, 13376 Marseille Cedex 12, France*

[8]*CPPM, CNRS-IN2P3 and University Aix Marseille II, Case 907, 13288 Marseille Cedex 9, France*

[9]*University of Oxford Astrophysics, Denys Wilkinson Building, Keble Road, Oxford OX1 3RH, UK*

The acceleration of the expansion of the universe, and the need for Dark Energy, were inferred from the observations of Type Ia supernovae (SNe Ia)[1;2]. There is consensus that SNe Ia are thermonuclear explosions that destroy carbon-oxygen white dwarf stars that accrete matter from a companion star[3], although the nature of this companion remains uncertain. SNe Ia are thought to be reliable distance indicators because they have a standard amount of fuel and a uniform trigger — they are predicted to explode when the mass of the white dwarf nears the Chandrasekhar mass[4] — 1.4 solar masses. Here we show that the high redshift supernova SNLS-03D3bb has an exceptionally high luminosity and low kinetic energy that both imply a *super*-Chandrasekhar mass progenitor. Super-Chandrasekhar mass SNe Ia should preferentially occur in a young stellar population, so this may provide an explanation for the observed trend that overluminous SNe Ia only occur in young environments[5;6]. Since this supernova does not obey the relations that allow them to be calibrated as standard candles, and since no counterparts have been found at low redshift, future cosmology studies will have to consider contamination from such events.

SNLS-03D3bb (SN 2003fg) was discovered on April 24, 2003 (UT) as part of the Supernova Legacy Survey (SNLS). Its redshift is $z = 0.2440 \pm 0.0003$, determined from host galaxy [OII], [OIII], Hα, and Hβ emission lines. A finding chart and observational details can be found in the supplementary information (SI). From the lightcurve (Figure 1) we measure a peak magnitude in the rest frame V band, $V = 20.50 \pm 0.06$ mag. This corresponds to an absolute magnitude of $M_V = -19.94 \pm 0.06$ ($H_0 = 70$ km s^{-1} Mpc^{-1}, $\Omega_M = 0.3$, flat universe). SNLS-03D3bb falls completely outside of the M_V distribution of low-z SNe Ia[7], and is 0.87 mag (a factor of 2.2)

brighter than the median. Note that neither changes in the Hubble constant nor Ω_M significantly affect this brightness difference. Asphericity may account for variations in SN Ia luminosity at the 25% level, but not a factor of two[8;9]. SNLS-03D3bb also does not follow the lightcurve width-luminosity relationship[10] for SNe Ia that allows them to be calibrated as standard candles — it is too bright for its lightcurve width ("stretch", s=1.13) by 0.61 ± 0.14 mag (4.4σ).

Type Ia supernovae are powered exclusively by the decay of ^{56}Ni and its decay product ^{56}Co [11], requiring ~ 0.6 $M_\odot$ of ^{56}Ni to reproduce a normal SNe Ia[12;13;14;15]. Since SNLS-03D3bb is 2.2 times overluminous, this implies that it has ~ 1.3 $M_\odot$of ^{56}Ni. Such a large ^{56}Ni mass is not possible if the progenitor is limited to the Chandrasekhar mass (1.4 $M_\odot$). Even models that burn the entire 1.4 $M_\odot$ to nuclear statistical equilibrium via a pure detonation produce only 0.92 $M_\odot$ of ^{56}Ni, with the remainder comprising other iron-peak elements[16]. Since at least 40% of the SN Ia must be elements other than ^{56}Ni to reproduce observed spectra[14;17], this implies a WD mass of ~ 2.1 $M_\odot$. Some authors find rapid rotation may support such a massive white dwarf[18]. The merger of two massive white dwarfs could also produce a super-Chandrasekhar product[19;20].

This simple estimation of the nickel mass is supported by a more detailed calculation using the principle that the luminosity at maximum light is proportional to the instantaneous rate of radioactive decay[21;22]. The impied Ni mass is[23;24]: $M_{\rm Ni} = \frac{L_{\rm bol}}{\alpha \dot{S}(t_R)}$, where $L_{\rm bol}$ is the bolometric luminosity at maximum light (the luminosity integrated from the ultraviolet to the infrared), and α is the ratio of bolometric to radioactivity luminosities, near unity. $\dot{S}$ is the radioactivity luminosity per solar mass of ^{56}Ni from its decay to ^{56}Co and subsequent decay to ^{56}Fe:

$\dot{S} = 6.31 \times 10^{43} e^{-t_R/8.8} + 1.43 \times 10^{43} e^{-t_R/111}$ erg s^{-1} M$_\odot^{-1}$, where t_R is the time in days for the supernova to rise from explosion to maximum light. Using $t_R = s \times 19.5$ days[25], for SNLS-03D3bb, $t_R = 22$ days (see SI for the effect of a shorter rise). We use $\alpha = 1.2$ as a conservative value, although for high ^{56}Ni masses, α may be lower, since nickel above the photosphere will not contribute to the luminosity[23].

To convert our V magnitude into a bolometric equivalent, we use a synthetic spectrum calculated to match the observed UV+optical spectrum (Fig. 3), but extended into the infrared (13% of the bolometric luminosity is from the IR extrapolation). The bolometric correction ($m_{\rm bc}$) is 0.07 ± 0.03 mag, such that $M_{\rm bol} = M_V + m_{\rm bc} = -19.87 \pm 0.06$ mag. Using these numbers, we calculate $M_{\rm Ni} = 1.29 \pm 0.07$ M$_\odot$ for SNLS-03D3bb, in agreement with the simple scaling argument used earlier. The quoted error is from the statistical, k-correction, and bolometric correction errors added in quadrature. SNLS-03D3bb has a significantly larger bolometric luminosity and implied ^{56}Ni mass compared to low redshift SNe (Fig. 2).

SNLS-03D3bb also has an unusually low ejecta velocity, as shown in the Keck spetrum taken 2 days after maximum light (Fig. 3). With a SiII velocity of 8000 ± 500 km s^{-1}, it falls well outside the range of velocities seen for this feature at maximum light (Fig. 4). This is hard to understand in the Chandrasekhar mass model, which predicts *higher* velocities for more luminous SNe Ia, in contrast to the unusually *low* velocities in SNLS-03D3bb.

The kinetic energy (E_k) of a SN Ia arises from the difference between the nuclear energy (E_n) obtained from the synthesis of elements via fusion in the explosion and the binding energy

(E_b) of the white dwarf[13]. Thus the kinetic energy velocity is: $v_{\rm ke} = \sqrt{\frac{2(E_n - E_b)}{M_{\rm WD}}}$, where $M_{\rm WD}$ is the mass of the white dwarf. The binding energy of a 1.4 $\rm M_\odot$ C/O WD is 0.5×10^{51} ergs[14]. For a $2\rm M_\odot$ WD and a central density of 4×10^9 g cm^{-3}, the binding energy is 1.3×10^{51} ergs[18].

Since there are only three classes of elements in a SN Ia (iron-peak elements, intermediate mass elements (IME), and unburned carbon and oxygen), a simple model can be developed for the nuclear energy generation, E_n. Burning a mixture of equal parts carbon and oxygen to the iron peak produces $E_{\rm Fe} = 1.55 \times 10^{51}$ erg $\rm M_\odot{}^{-1}$, while the synthesis of ^{28}Si produces 76% as much energy[13]. Thus: $E_n = E_{\rm Fe} M_{\rm WD}(f_{\rm Fe} + 0.76 f_{\rm IME})$, where $M_{\rm WD}$ is in solar masses, and $f_{\rm Fe}$ and $f_{\rm IME}$ are the fractional compositions of iron peak and intermediate mass elements. If $f_{\rm Fe}$ and $f_{\rm IME}$ do not sum to one, the remainder is the fraction of unburned carbon and oxygen (f_C), which does not contribute to the nuclear energy. The ^{56}Ni makes up approximately 70% of iron-peak elements [14;16], so we adopt $M_{\rm Ni} = 0.7 M_{\rm WD} f_{\rm Fe}$, where $M_{\rm Ni}$ is the mass of ^{56}Ni.

In the Chandrasekhar mass model, more luminous SNe, with more ^{56}Ni, have a higher $v_{\rm ke}$ (Fig. 4). Increasing the fraction of unburned carbon and oxygen, f_C, can lower the kinetic energy, perhaps accounting for some of the dispersion in SN Ia velocities. However, this also lowers the available ^{56}Ni, so it cannot account for the low velocity seen in SNLS-03D3bb.

The kinetic energy gives the velocity of the supernova averaged over the entire mass, approximately equivalent to the velocity a few weeks after maximum light[13]. The most appropriate observational signature of this velocity is unclear, since SN Ia line velocities change with time, and different ions can have different relative velocities. We find good agreement between the

SiII velocity at 40 days after maximum light[26] and the theoretical kinetic energy velocity, but we emphasize that this is in imperfect comparison.

A super-Chandrasekhar mass reproduces the low velocities seen in SNLS-03D3bb (Fig. 4). Since Chandrasekhar models with more Ni produce higher velocities, the low velocities of SNLS-03D3bb imply an increased progenitor binding energy and thus a larger total mass. As a caveat, we note that this simple calculation is only intended to illustrate general trends. Future theoretical studies will have to assess such complications as using different ions, different white dwarf density structures, and a wider range of binding energies.

Super-Chandrasekhar mass SNe Ia should be more likely in a young stellar population, where the most massive stars exist[19;20]. The low mass, star forming host of SNLS-03D3bb is consistent with this scenario (see SI). Thus, the apparent existence of super-Chandrasekhar mass SNe Ia may explain why the most luminous SNe Ia only occur in young stellar environments[5;6]. The standard Chandrasekhar mass model offers no explanation for this behaviour, since the total amount of fuel and triggering mechanism should be independent of the mass of the progenitor stars.

SNe such as SNLS-03D3bb will have to be screened out in cosmological studies. Since younger stellar environments produce more luminous SNe, as the mean stellar age decreases with redshift the mean properties of SNe Ia will change[5]. This can be calibrated if all SNe obey the same stretch-luminosity relationship, but SNLS-03D3bb does not. Its peculiarity was so obvious that it was excluded from the SNLS cosmological result[7], but less extreme objects could lurk in SN samples. Future cosmology studies will have to carefully scrutinise SNe Ia from young populations

to see if they obey the same lightcurve shape-luminosity relationship as other SNe Ia.

1. Perlmutter, S. *et al.* Measurements of Omega and Lambda from 42 High-Redshift Supernovae. *Astrophys. J.* **517**, 565–586 (1999).

2. Riess, A. G. *et al.* Observational Evidence from Supernovae for an Accelerating Universe and a Cosmological Constant. *Astron. J.* **116**, 1009–1038 (1998).

3. Hoyle, F. & Fowler, W. A. Nucleosynthesis in Supernovae. *Astrophys. J.* **132**, 565–590 (1960).

4. Chandrasekhar, S. The Maximum Mass of Ideal White Dwarfs. *Astrophys. J.* **74**, 81–82 (1931).

5. Sullivan, M. *et al.* Rates and properties of type Ia supernovae as a function of mass and star-formation in their host galaxies. *Astrophys. J., in press* (2006). `astro-ph/0605455`.

6. Hamuy, M. *et al.* The Absolute Luminosities of the Calan/Tololo Type IA Supernovae. *Astron. J.* **112**, 2391–2397 (1996).

7. Astier, P. *et al.* The Supernova Legacy Survey: measurement of Ω_M, Ω_Λ and w from the first year data set. *Astron. & Astrophys.* **447**, 31–48 (2006).

8. Howell, D. A., Höflich, P., Wang, L. & Wheeler, J. C. Evidence for Asphericity in a Subluminous Type Ia Supernova: Spectropolarimetry of SN 1999by. *Astrophys. J.* **556**, 302–321 (2001).

9. Kasen, D., Nugent, P., Thomas, R. C. & Wang, L. Could There Be a Hole in Type Ia Supernovae? *Astrophys. J.* **610**, 876–887 (2004).

10. Phillips, M. M. The absolute magnitudes of Type IA supernovae. *Astrophys. J. Lett.* **413**, L105–L108 (1993).

11. Colgate, S. A. & McKee, C. Early Supernova Luminosity. *Astrophys. J.* **157**, 623–644 (1969).

12. Woosley, S. E. & Weaver, T. A. The physics of supernova explosions. *Ann. Rev. Astron. Astrophys.* **24**, 205–253 (1986).

13. Branch, D. The Hubble constant from nickel radioactivity in type IA supernovae. *Astrophys. J.* **392**, 35–40 (1992).

14. Nomoto, K., Thielemann, F.-K. & Yokoi, K. Accreting white dwarf models of Type I supernovae. III - Carbon deflagration supernovae. *Astrophys. J.* **286**, 644–658 (1984).

15. Hoflich, P. Analysis of the type IA supernova SN 1994D. *Astrophys. J.* **443**, 89–108 (1995).

16. Khokhlov, A., Mueller, E. & Hoeflich, P. Light curves of Type IA supernova models with different explosion mechanisms. *Astron. & Astrophys.* **270**, 223–248 (1993).

17. Fisher, A., Branch, D., Hatano, K. & Baron, E. On the spectrum and nature of the peculiar Type IA supernova 1991T. *MNRAS* **304**, 67–74 (1999).

18. Yoon, S.-C. & Langer, N. On the evolution of rapidly rotating massive white dwarfs towards supernovae or collapses. *Astron. & Astrophys.* **435**, 967–985 (2005).

19. Tutukov, A. V. & Yungelson, L. R. Merging of Binary White Dwarfs Neutron Stars and Black-Holes Under the Influence of Gravitational Wave Radiation. *MNRAS* **268**, 871–879 (1994).

20. Howell, D. A. The Progenitors of Subluminous Type Ia Supernovae. *Astrophys. J. Lett.* **554**, L193–L196 (2001).

21. Arnett, W. D. Type I supernovae. I - Analytic solutions for the early part of the light curve. *Astrophys. J.* **253**, 785–797 (1982).

22. Arnett, W. D., Branch, D. & Wheeler, J. C. Hubble's constant and exploding carbon-oxygen white dwarf models for Type I supernovae. *Nature* **314**, 337–338 (1985).

23. Nugent, P. *et al.* Low Hubble Constant from the Physics of Type Ia Supernovae. *Physical Review Letters* **75**, 394–397 (1995).

24. Nugent, P. E. Non-Local Thermodynamic Equilibrium Spectrum Synthesis of Type IA Supernovae. *Ph.D. Thesis* (1997).

25. Conley, A. *et al.* The rise time of Type Ia supernovae from the Supernova Legacy Survey. *Astron. J., submitted* (2006).

26. Benetti, S. *et al.* The Diversity of Type Ia Supernovae: Evidence for Systematics? *Astrophys. J.* **623**, 1011–1016 (2005).

27. Nugent, P., Kim, A. & Perlmutter, S. K-Corrections and Extinction Corrections for Type Ia Supernovae. *PASP* **114**, 803–819 (2002).

28. Bessell, M. S. Ubvri passbands. *PASP* **102**, 1181–1199 (1990).

29. Fisher, A., Branch, D., Nugent, P. & Baron, E. Evidence for a High-velocity Carbon-rich Layer in the Type IA SN 1990N. *Astrophys. J. Lett.* **481**, L89–L92 (1997).

30. Marion, G. H. *et al.* Low Carbon Abundance in Type Ia Supernovae. *ArXiv Astrophysics e-prints* (2006). `arXiv:astro-ph/0601614`.

Supplementary Information is linked to the online version of this paper at www.nature.com/nature.

Acknowledgements SNLS relies on observations with MegaCam, a joint project of CFHT and CEA/DAPNIA, at the Canada-France-Hawaii Telescope (CFHT). We used data products produced at the Canadian Astronomy Data Centre as part of the CFHT Legacy Survey. Some data were obtained at the W.M. Keck Observatory. We acknowledge support from NSERC, NERSC, CIAR, CNRS/IN2P3, CNRS/INSU, CEA, and the DOE.

Author Infomation Reprints and permissions information is available at npg.nature.com/reprintsandpermissions. The authors declare no competing financial interests. Correspondence and requests for materials should be addressed to D.A.H (howell@astro.utoronto.ca).

Figure 1 The lightcurve of SNLS-03D3bb. We fit k-corrected[27] template lightcurves to the observed photometry of SNLS-03D3bb, then transform the peak magnitudes back to the Johnson-Cousins[28] BV magnitudes in the Vega system. We find peak magnitudes of $B = 20.35$ mag and $V = 20.50 \pm 0.06$ mag from a simultaneous fit to g' and r' data. The error (s.d.) consists of 0.04 statistical error and 0.04 k-correction error. A lightcurve template was fit using the stretch method[1] (stretching the time axis of a template lightcurve by a stretch factor, $s = 1.13$). The epoch of maximum light relative to the rest frame B band was determined from a simultaneous fit to all of the data. At maximum, we only use the V band value to compare to other SNe, since it is the best constrained. Data past +35 days was not used in the fit. The arrows are three sigma upper limits.

Figure 2 Bolometric luminosity vs. implied $^{56}\mathrm{Ni}$ mass for SNLS-03D3bb and low redshift SNe Ia[7]. The low redshift SNe Ia were fit using the same techniques as those used for SNLS-03D3bb: the bolometric luminosity was determined using the peak magnitude in the V band from a simultaneous fit to B and V band data. A bolometric correction of 0.06 mag was adopted for low redshift SNe Ia, obtained by integrating the $s = 1$ k-correction template[27]. A 0.05 mag k-correction plus bolometric correction error (s.d.) is shown for the low redshift SNe Ia. The solid line represents a normal stretch=1 SN Ia, with a rise time (t_r) of -19.5 days, while dotted lines show $s = 0.9$ ($t_r = 17.6$) and $s = 1.1$ ($t_r = 21.5$). Low luminosity SNe Ia have lower stretches, and thus shorter rise times, resulting in less $^{56}\mathrm{Ni}$ for a given luminosity, while high stretch SNe Ia show opposite behaviour. The dashed

line shows an upper limit for the expected $^{56}\mathrm{Ni}$ mass in a Chandrasekhar mass SN Ia, obtained by burning the entire white dwarf to iron-peak elements in a detonation[16].

Figure 3 Keck LRIS spectrum of SNLS-03D3bb at 2 days after maximum light compared to a spectrum of the normal Type Ia SN 1994D. Also plotted is a SYNOW fit to the data with dominant ions labeled. SYNOW is a parameterized resonance-scattering code, allowing the user to adjust optical depths, temperatures, and velocities to aid in the identification of supernova lines[29]. SYNOW parameters are listed in the supplementary information. SNLS-03D3bb shows the lines of IMEs typically seen in a SN Ia at maximum light — SiII, SII, and CaII, but in SNLS-03D3bb the velocity of the lines is lower than usual. The line at 415 nm appears to be CII, but the other predicted carbon features cannot be clearly identified due to the lower signal-to-noise ratio of the spectrum in the red. No other identification could be found for the 415 nm feature.

Figure 4 Inferred Ni mass vs. SiII 615 nm velocity. **a**, The data at maximum light[26]. Ni masses are converted as described in the text using $M_{\mathrm{bol}} = M_B + 0.2$. Filled circles are from early type galaxies (E or S0), while open circles are from late type galaxies (Sa-Irr). Circle size is proportional to $v_{\mathrm{Si}}/\dot{v}_{\mathrm{Si}}$, where $\dot{v}_{\mathrm{Si}}$ is the rate of change of the velocity of the SiII feature. There is no $\dot{v}_{\mathrm{Si}}$ measurement for SNLS-03D3bb. **b**, Kinetic energy velocity of SNe Ia versus Ni mass for 1.4 solar mass models with different fractions of unburned carbon (f_C). This unburned fraction should not be much higher than $\sim 20\%$ because carbon is rarely seen in SN Ia spectra[30]. Overplotted symbols are v_{Si} for low redshift SNe

Ia[26] extrapolated to 40 days after maximum (correcting for stretch). For SNLS-03D3bb we use $\dot{v}_{\rm Si}$ from its closest neighbor. The error bar reflects the range if an average value of $\dot{v}_{\rm Si}$ is used. SNLS-03D3bb is not consistent with the 1.4 $\rm M_\odot$ model. **c**, As above, but showing that $M_{\rm WD} \sim 2\ \rm M_\odot$ models can explain SNLS-03D3bb. Less extreme super-Chandrasekhar mass models are consistent with the low redshift data. The three low $^{56}\rm Ni$ SNe are not necessarily super-Chandrasekhar SNe Ia — their large values of $\dot{v}_{\rm Si}$ make projections to 40 days uncertain.

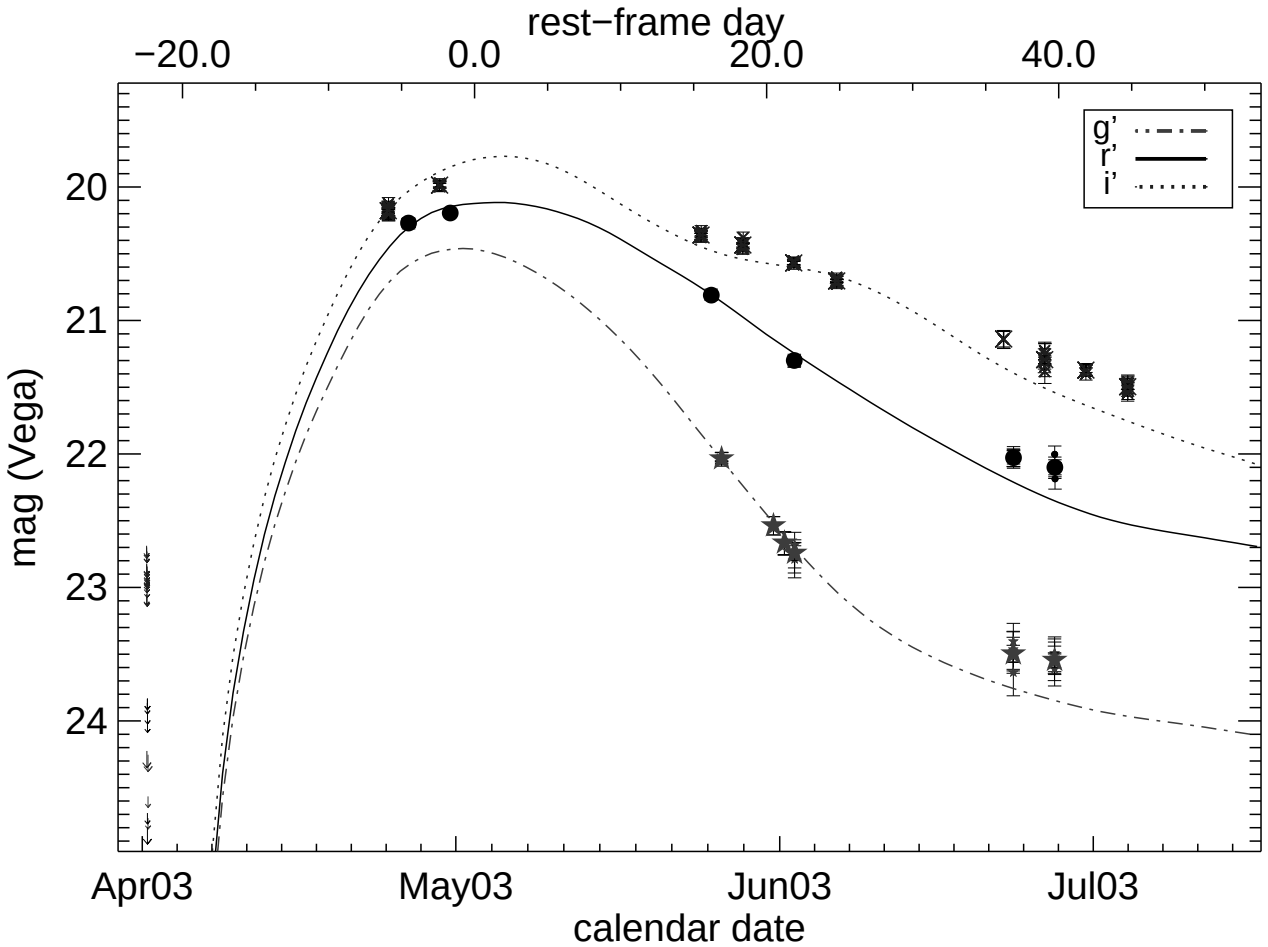
rest−frame day
−20.0
0.0
20.0
40.0
g'
r'
i'
mag (Vega)
20
21
22
23
24
Apr03
May03
Jun03
Jul03
calendar date

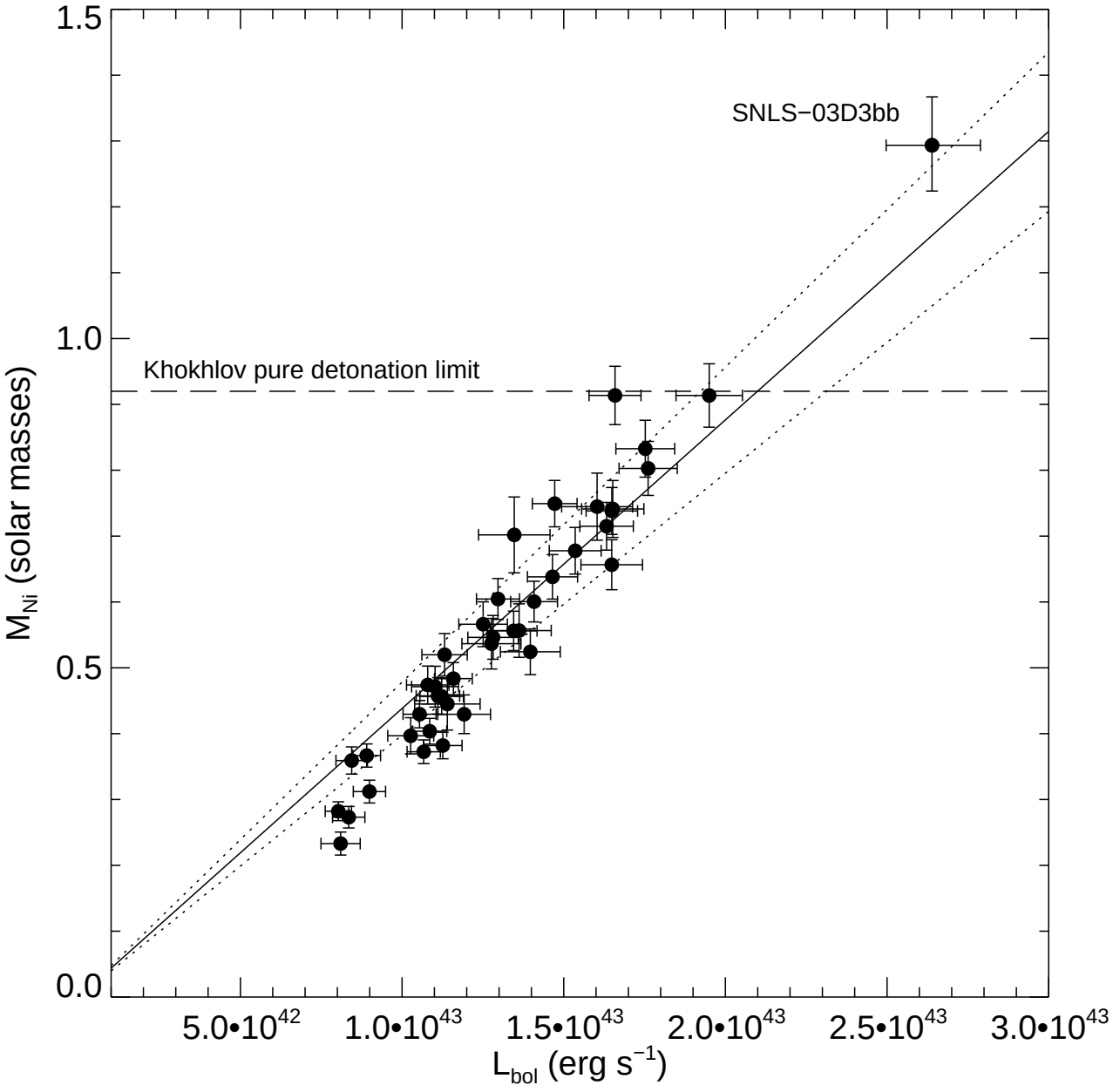
1.5
1.0
0.5
0.0
SNLS−03D3bb
Khokhlov pure detonation limit
M_{Ni} (solar masses)
5.0•10^42
1.0•10^43
1.5•10^43
2.0•10^43
2.5•10^43
3.0•10^43
L_{bol} (erg s^{-1})

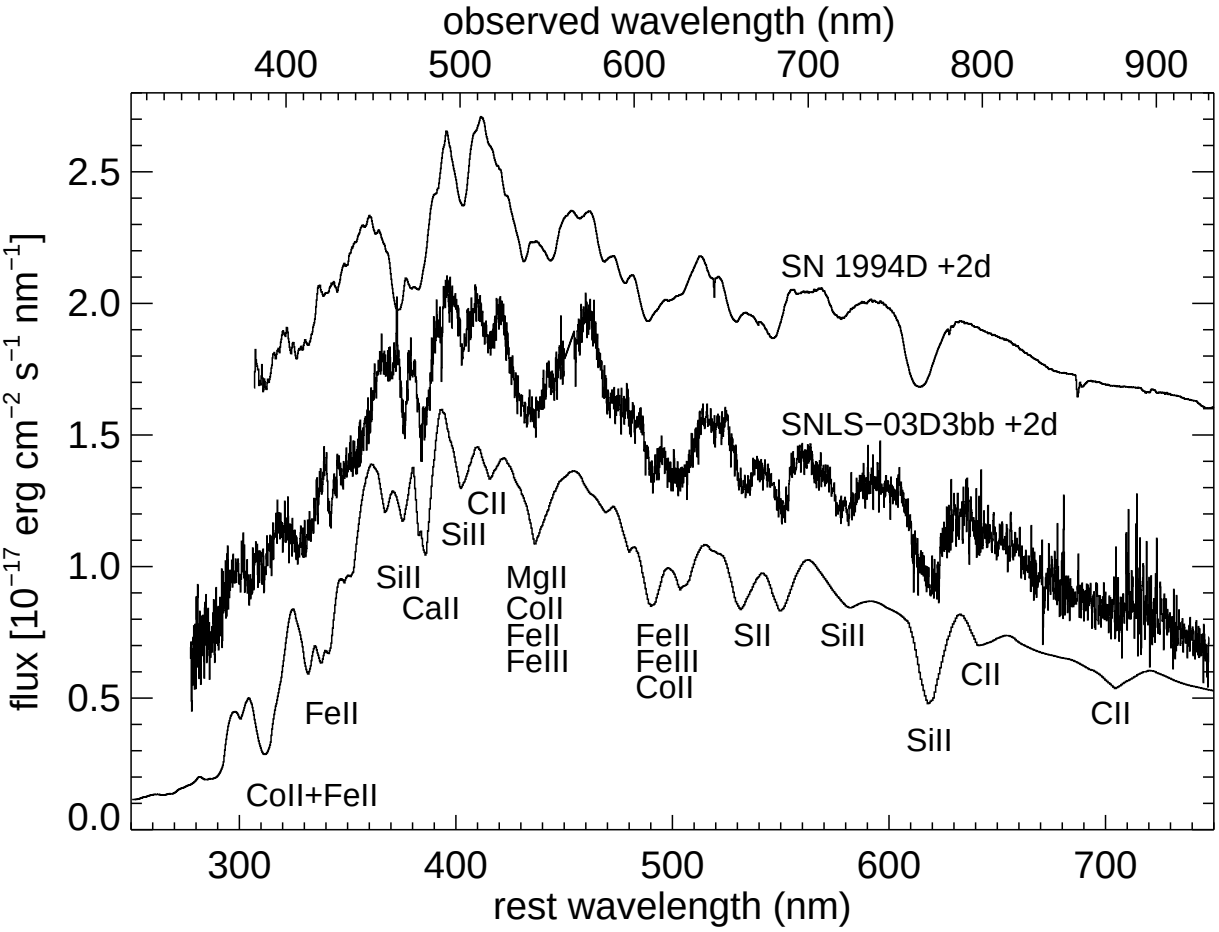
observed wavelength (nm)
400
500
600
700
800
900
flux [10^-17 erg cm^-2 s^-1 nm^-1]
0.0
0.5
1.0
1.5
2.0
2.5
SN 1994D +2d
SNLS−03D3bb +2d
CaII
SiII
CII
SiII
MgII
CoII
FeII
FeIII
FeII
FeIII
CoII
SII
SiII
SiII
CII
CII
FeII
CoII+FeII
300
400
500
600
700
rest wavelength (nm)

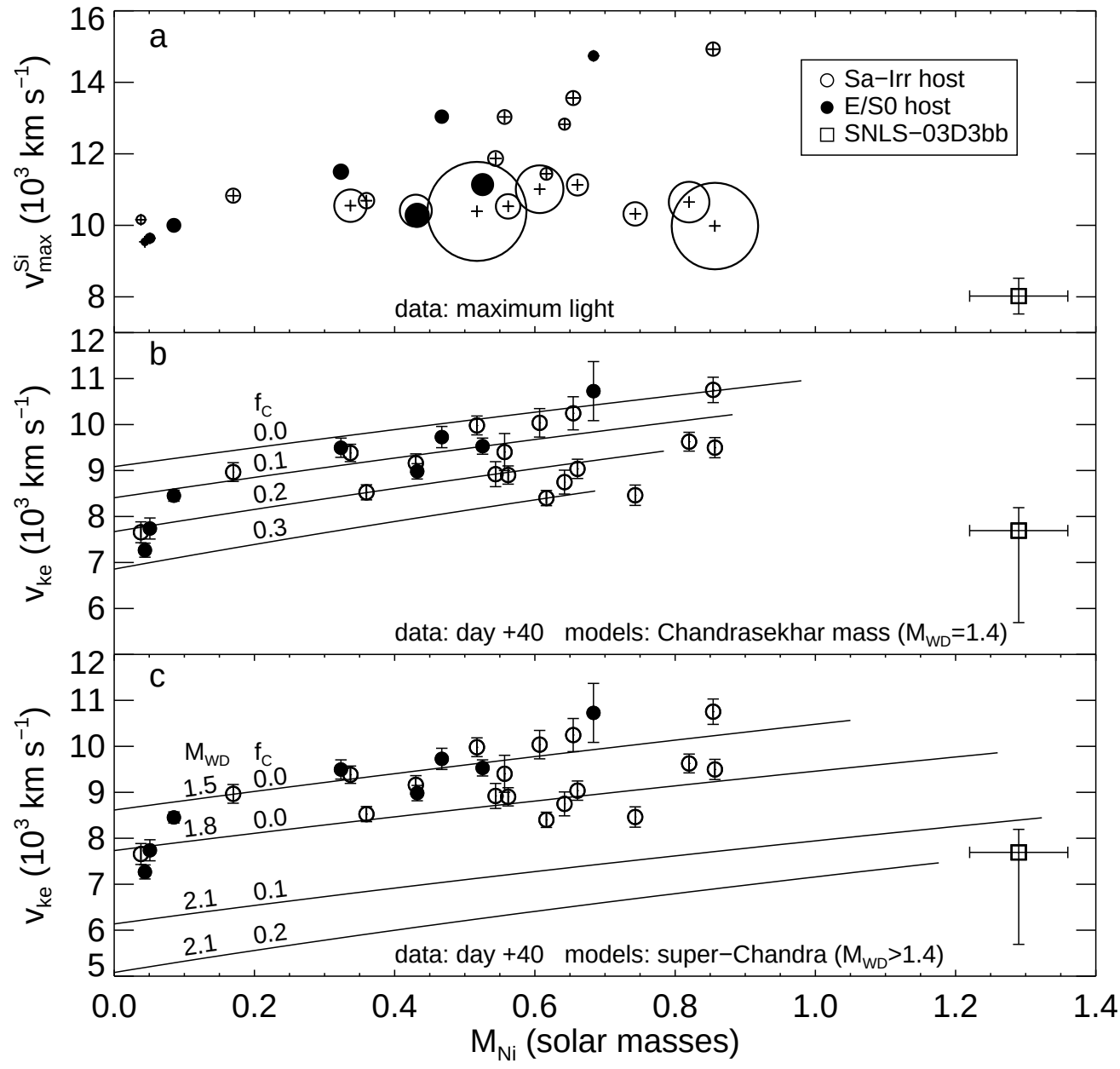
a
Sa−Irr host
E/S0 host
SNLS−03D3bb
data: maximum light
b
f_C
0.0
0.1
0.2
0.3
data: day +40 models: Chandrasekhar mass (M_{WD}=1.4)
c
M_{WD} f_C
1.5 0.0
1.8 0.0
2.1 0.1
2.1 0.2
data: day +40 models: super−Chandra (M_{WD}>1.4)
v^{Si}_{max} (10^3 km s^{-1})
v_{ke} (10^3 km s^{-1})
M_{Ni} (solar masses)

SN Location SNLS-03D3bb is located at RA: 14:16:18.920 Dec: +52:14:53.66 (J2000) in the D3 (extended Groth Strip) field of the Supernova Legacy Survey (SNLS), located in a satellite galaxy to a larger tidally distorted spiral (Supplementary Figure 1). The SN is 0.18″W and 0.03″S from the centre of its host and 4.04″E and 2.53″S from the centre of the larger galaxy.

Spectroscopy Spectroscopic observations were obtained on 2003 May 6.3 at Keck I using the Low Resolution Imaging Spectrograph (LRIS) in with a 1″ slit, placed at a 261° position angle to get the redshift of the faint host and the large nearby galaxy. From the two dimensional spectrum it is apparent that both galaxies are at the same redshift. Two 1000 second observations were taken, dithering between observations. The 560 dichroic was used to split the observations between the grism on the blue side (600 lines at 400 nm) and the grating on the red side (400 lines grating blazed at 850 nm with central wavelength 725 nm).

Follow-up photometric observations were obtained during the "presurvey" commissioning phase of the SNLS. Basic photometric reductions were done using the Elixir pipeline, and deep reference images containing no supernova light were subtracted from each image to remove galaxy contamination. PSF-photometry was done on the difference image.

At day 20 after maximum brightness, where the colors are well measured, SNLS-03D3bb has $B - V = 0.74$, and $V - R = 0.16$, within the distribution of local SNe Ia. There is no evidence that the SN Ia is significantly reddened from dust, but we do not know the instrinsic color of such an odd SN Ia. Any extinction correction would make the SN Ia intrinsically more luminous, and thus require a higher white dwarf mass.

SYNOW fit The best fit SYNOW parameters were a photospheric velocity of 8000 km s^{-1} with a maximum velocity of 12,500 km s^{-1} (except for Ca II at 10,000 km s^{-1}) and a underlying blackbody temperature of 9000 K (varried by ± 2500 K in the IR to account

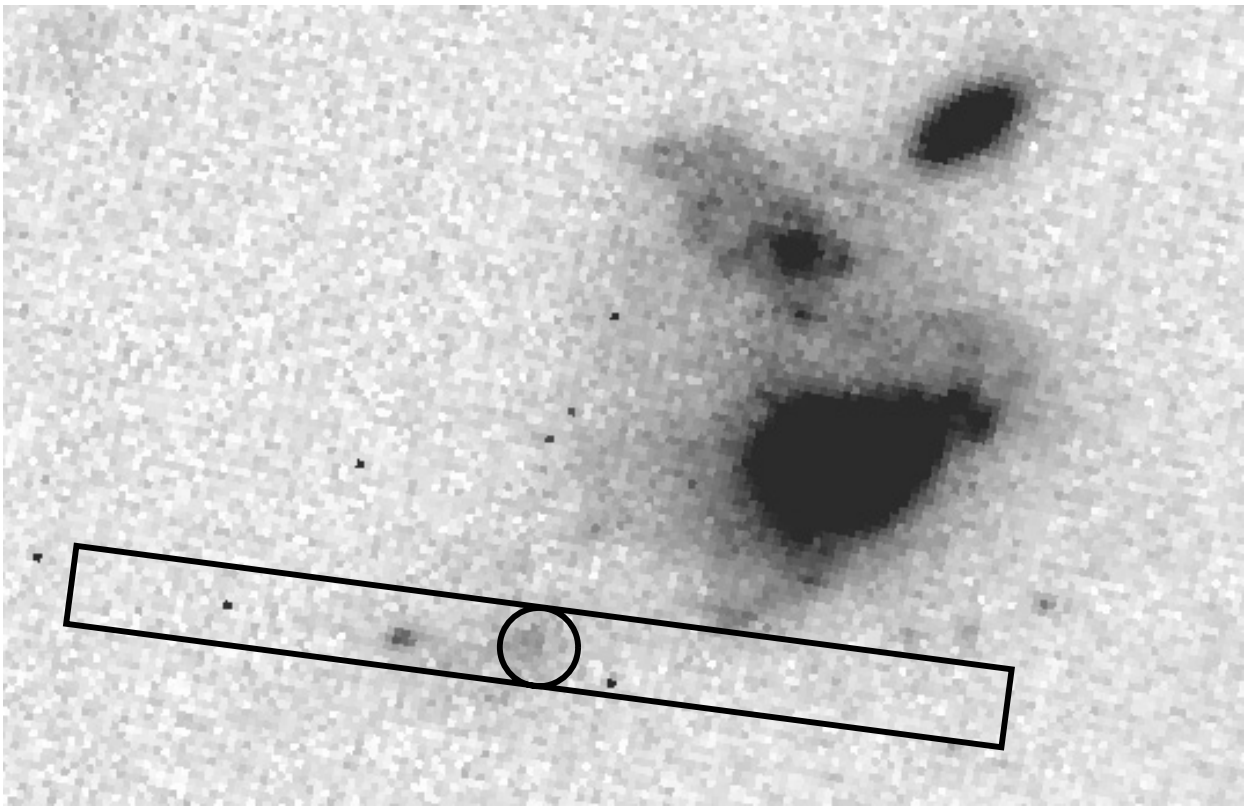

Fig. 1.— A Hubble Space Telescope ACS image of the host galaxy of SNLS-03D3bb taken through the F814W filter. Though the supernova is not present in this image, the circle marks its position. The spectroscopic slit was placed at 261° to get the redshifts of both the small host and the larger neighboring galaxy. Both are at $z = 0.2440$.

for uncertainties in the bolometric correction). The excitation temperature was 10,000 K for all ions except C II, which was placed at 35,000 K in order to get relative line strengths correct in the spectrum. This is similar to what was used in a preliminary fit to SN 2006D which showed 4 C II lines in the spectrum.

Alternative explanations It is possible to lower the implied Ni mass by decreasing t_R in Equation 2, i.e. by shortening the time from explosion to maximum light. However, to get 0.9 $M_\odot$ of ^{56}Ni would require $t_R = 14.6$ days, 66% of the rise time inferred from the post maximum decline. Such a fast rise and slow decline has never before been seen in a SN Ia, so we consider this possibility to be highly unlikely.

Another way to decrease the implied Ni mass for SNLS-03D3bb is asymmetry. Spectropolarimetric observations imply that some SNe Ia are aspherical[1] [2] [3] [4], perhaps giving rise to a direction-dependent deviations in brightness. However, such brightness deviations amount to only a few tenths of a magnitude. No theoretical model predicts a factor of two increase in brightness due to viewing a SN Ia from a preferred geometry. The relative rarity of SNLS-03D3bb offers another constraint. The fact that this type of object has been seen only once out of hundreds of supernova observations implies that if such behaviour is common, the area of increased luminosity must have a small solid angle. This might be possible if we were looking down a jet, but SNLS-03D3bb has unusually low, not unusually high velocities.

Young population Super-Chandrasekhar white dwarfs should be more likely in a young stellar population[5] [6]. The two white dwarfs in a double degenerate system must have a total mass above the Chandrasekhar limit if the secondary (by definition the lower mass star) is larger than 0.7 solar masses. Stars with an initial mass above 3 $M_\odot$ produce white dwarfs larger than 0.7 $M_\odot$[7]. Since it takes 900 million years for a 3 $M_\odot$ star to evolve off the main sequence[8], all white dwarf pairs created before 900 million years must have

a combined mass above the Chandrasekhar mass. In the single degenerate scenario, the massive hydrogen envelopes of secondaries and higher starting primary white dwarf mass also make super-Chandrasekhar masses easier to achieve in a young population. Populations older than a few Gyr are a factor of 10–20 are less efficient than younger populations at creating even a Chandrasekhar mass white dwarf through the single degenerate path.[9] This inefficiency would increase if a super-Chandrasekhar white dwarf is required.

To estimate the age of the host galaxy of SNLS-03D3bb, we fit PEGASE.2 population synthesis models to the host galaxy $u^*g'r'i'z'$ photometry[1]0. We find log $M_{gal} = 8.93^{+0.81}_{-0.50}$, where M_{gal} is the host galaxy stellar mass in $M_\odot$; the galaxy is less than a tenth the mass of the Milky Way. We find a star formation rate of $1.26^{+0.02}_{-1}$ $M_\odot$ yr^{-1}, averaged over 0.5 Gyr. This formally implies an age of $\sim$ 700 Myr, though the unknown star formation history of the galaxy makes a precise determination impossible. We treat this only as an indicator of a young stellar population, confirming that SNLS-03D3bb matches environmental expectations.

Table 1. Photometry of SNLS-03D3bb

MJD	Exptime	Flux	Flux Error	Mag	Filter
52721.62	720.6	1.302e-19	1.4e-19	24.88	g
52722.59	720.7	-3.566e-19	1.1e-19	25.16	g
52730.55	360.3	1.487e-19	1.4e-19	24.88	g
52785.43	900.9	7.926e-18	5.6e-20	22.03	g
52790.39	180.2	4.994e-18	1.5e-19	22.54	g
52791.44	360.4	4.434e-18	1.6e-19	22.66	g
52792.41	720.6	4.131e-18	9.7e-20	22.74	g
52813.34	720.7	2.131e-18	6.8e-20	23.46	g
52817.29	900.8	1.983e-18	5.3e-20	23.54	g
52721.57	1801.7	-2.021e-20	5.1e-20	25.21	r
52730.48	1080.7	-4.511e-20	5.0e-20	25.23	r
52755.46	2702.7	1.932e-17	4.6e-20	20.26	r
52759.46	720.8	2.072e-17	7.7e-20	20.19	r
52784.44	1800.9	1.176e-17	5.6e-20	20.80	r
52792.38	1801.0	7.486e-18	4.6e-20	21.29	r
52813.36	1440.7	3.814e-18	5.4e-20	22.03	r
52817.31	1173.3	3.583e-18	3.9e-20	22.09	r
52721.52	3603.6	-6.529e-20	2.8e-20	25.17	i
52723.57	2702.5	-7.554e-21	4.7e-20	24.61	i
52730.41	3781.7	-1.297e-19	3.7e-20	24.88	i
52753.52	3424.4	1.118e-17	6.9e-20	20.17	i

1. Howell, D. A., Höflich, P., Wang, L., & Wheeler, C. Evidence for Asphericity in a Subluminous Type Ia Supernova: Spectropolarimetry of SN 1999by. *Astrophys. J.* **556**, 302—321 (2001).

2. Kasen, D., Nugent, P., Thomas, R. C., & Wang, L. Coult there be a hole in Type Ia Supernovae? *Astrophys. J.* **610**, 876—887 (2004).

3. Wang, L. et al. Spectropolarimetry of SN 2001el in NGC 1448: Asphericity of a Normal Type Ia Supernova. *Astrophys. J.* **591**, 1110—1128 (2003).

4. Leonard, D., Li, W.-D., Filippenko, A. V., Foley, R., & Chornock, R. Evidence for Spectropolarimetric Diversity in Type Ia Supernovae. *Astrophys. J.* **635**, 450—475 (2005).

5. Tutukov, A. V. & Yungelson, L. R. Merging of Binary White Dwarfs Neutron Stars and Black Holes Under Gravitational Wave Radiation *MNRAS* **268**, 871—879 (1994)

6. Howell, D. A. The Progenitors of Subluminous Type Ia Supernovae *Astrophys. J. Lett.* **556**, 193—196 (2001)

7. Ferrario, L., Wickramasinghe, D., Liebert, J., & Williams, K. A. The open-cluster initial-final mass relationship and the high-mass tail of the white dwarf distribution. *MNRAS* **361**, 1131—1135 (2005).

8. Girardi, L., Bressan, A., Bertelli, G., & Chiosi, C. Evolutionary tracks and isochrones of low- and intermediate-mass stars: From 0.15 to 7 $M_{\odot}$ and from Z=0.0004 to 0.03 *Astron. & Astrophys. Sup.*, **141**, 371–383 (2000)

9. Greggio, L. The rates of Type Ia supernovae. I. Anylytical formulations. *Astron. & Astrophys.*, **441**, 1055-1078 (2005). 10. Sullivan, M. et al. Rates and properties of Type Ia supernovae as a function of mass and star formation rate in their host galaxies. *Astrophys. J., in press*, (2006)

Table 1—Continued

MJD	Exptime	Flux	Flux Error	Mag	Filter
52758.43	1441.4	1.333e-17	6.0e-20	19.98	i
52783.45	3641.2	9.458e-18	6.5e-20	20.35	i
52787.46	3641.1	8.827e-18	6.9e-20	20.43	i
52792.32	3641.2	7.796e-18	4.4e-20	20.56	i
52796.43	3641.1	6.916e-18	4.0e-20	20.69	i
52812.39	1040.3	4.612e-18	2.2e-19	21.13	i
52816.33	3641.4	4.007e-18	6.7e-20	21.28	i
52820.28	3120.6	3.723e-18	3.3e-20	21.36	i
52824.28	3641.2	3.317e-18	3.6e-20	21.49	i